Macromolecules

pubs.acs.org/Macromolecules Article

Influence of Network Topology on the Viscoelastic Properties of Double Dynamics Hydrogels

Hui Yang, Evelyne van Ruymbeke,* and Charles-André Fustin*

Cite This: https://doi.org/10.1021/acs.macromol.2c00712 Read Online

ACCESS | Metrics & More | Article Recommendations | Supporting Information

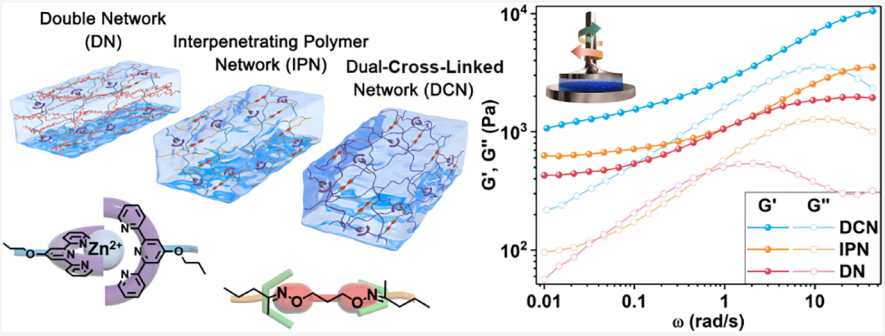

ABSTRACT: Dual-cross-linked networks (DCNs), interpenetrating polymer networks (IPNs), and IPN-derived double networks (DNs) are increasingly utilized to fabricate hydrogels with unique mechanical properties. However, the relationship between the topology of these networks and the resulting dynamics is rarely compared and little understood. To tackle this shortcoming, this work presents a systematic investigation of the viscoelastic properties of DCN, IPN, and DN hydrogels as well as their corresponding single networks by oscillatory shear rheology using both frequency and strain sweeps. All the hydrogels are based on the same orthogonal combination of a supramolecular interaction: zinc(II)-terpyridine bis-complexes, and of a reversible covalent bond: oxime, as cross-links. To understand the contribution of each sub-network to the properties of the DCN, IPN, and DN hydrogels, the corresponding single networks, i.e., cross-linked by only one type of bond, are first studied in detail. All double dynamics hydrogels have a plateau modulus much higher than the sum of the plateau modulus of the single networks, evidencing a synergetic effect between the sub-networks. However, the origin of this modulus increase varies according to the network topology. We also show that the relaxation behaviors of the DCN, IPN, and DN hydrogels are influenced by the dynamics of the corresponding single dynamic networks. Finally, the strain sweeps reveal that, for all network topologies, the amplitude of deformation at which the linear viscoelastic region of the double dynamics networks stops is governed by the oxime network, while the metallo-supramolecular network governs the amplitude of deformation up to which the sample can resist before starting to break.

INTRODUCTION

As prominent soft and wet materials, hydrogels have been extensively studied to tailor and adapt them for emerging fields of advanced applications such as nanogenerators,[1] soft robots,[2] 3D and 4D printing,[3] wearable and implantable devices,[4] artificial muscle, and skin and nerve.[5−7] These hydrophilic cross-linked three-dimensional macromolecular network structures can indeed exhibit a variety of application-relevant properties such as stimuli-responsiveness, self-healing, stress relaxation, and shape memory.[8] The high water content not only brings fluidity and transparency to the polymer hydrogels but also entails fragility of the materials, which restricts the scope of their practical applications in real life. Aiming to address this shortcoming, two major strategies have been adopted to improve the mechanical properties of polymer hydrogels: introducing a variety of cross-links and modifying the network topology.[9]

On the facet of cross-links, dynamic bonds, comprising dynamic covalent bonds (DCBs) and supramolecular interactions, have been widely embedded into polymeric networks, often to study the relationships between the bond strength and kinetics and the macroscopic rheological and mechanical properties of the materials.[10,11] In general, DCBs (e.g., imine, acylhydrazone, oxime, and disulfide) are stable covalent bonds under ambient conditions, but their dynamics can be activated by stimuli such as pH, heat, light, or stress.[12] In some cases (e.g., boronic esters), the DCB exchange/association/dissoci-

Received: April 7, 2022
Revised: May 12, 2022

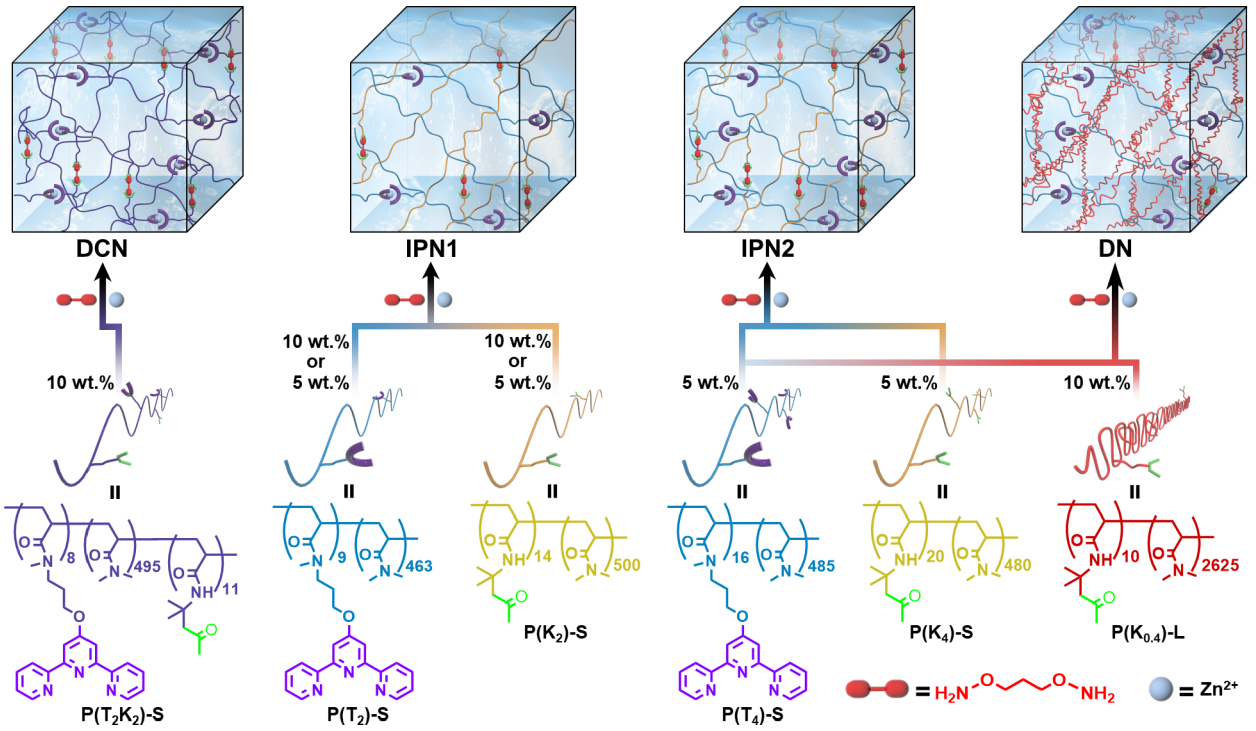

Figure 1. Schematic representation of dual-cross-linked network (DCN), interpenetrating polymer network (IPN), and double network (DN) hydrogels prepared by cross-linking various random copolymers bearing ketone (K) and/or terpyridine (T) groups by formation of oxime bonds and zinc(II)-terpyridine bis-complexes (Zn^{2+}-Tpy).

ation kinetics can be expressed even in the absence of a stimulus.[13] Unlike DCBs, supramolecular interactions including hydrogen bonding, metal−ligand coordination, pi-pi stacking, etc., are often more dynamic even under ambient conditions, being able to undergo rapid exchange, and have been widely used to build supramolecular polymers and networks.[14] Compared to the use of a single type of dynamic bond, the combination of robust and adaptable DCBs with more dynamic supramolecular interactions is a promising strategy for engineering the next generation of smart polymeric materials exhibiting unusual viscoelastic characteristics such as a tunable time-dependent mechanical modulus,[15] adjustable stress relaxation,[16] shear-thinning properties,[17] and combining enhanced toughness[18,19] and stimuli-responsiveness[20] with efficient self-healing.[21]

As for the network topology of hydrogels, dual-cross-linked networks (DCNs), interpenetrating polymer networks (IPNs), and double networks (DNs) are highlighted strategies for preparing polymer hydrogels with enhanced mechanical properties.[22] A dual-cross-linked network (DCN), which is also called the dual network[23] or dual-cross-linked single network,[24] is a network usually composed of only one polymer[25−27] cross-linked by two types of bonds, one of them at least being a dynamic bond. Interpenetrating polymer networks (IPNs) are generally made of two or more interlaced macromolecular networks that are independent, i.e., having no covalent bonds between each other.[28,29] Double networks (DNs)[30] are a special subset of IPNs and comprise two asymmetric sub-networks: the first sacrificial network is highly cross-linked and provides energy dissipation, and the interpenetrated second network is loosely cross-linked to insure shape persistence and to impart elasticity.[31]

The two above strategies, i.e., using different types of (dynamic) cross-links and adapting network topology, have also been combined to further tune the hydrogel properties and impart them with reversibility and stimuli responsiveness.[32,33] However, the synergetic effects between these two categories of cross-links on the viscoelastic behaviors of gels are rarely studied in detail, not to mention the interplay with the network architecture. For example, Zhang and co-workers investigated dual network elastomers based on boronic ester dynamic covalent bonds and quadruple hydrogen bonds as cross-links in poly(*n*-butyl acrylate) (PnBA).[34] They showed that networks based only on boronic esters can start to flow at intermediate times, while networks based on the strong quadruple hydrogen bonds partially relax but do not flow even at long times. The relaxation behavior of the dual network on the other hand is largely dominated by the strong quadruple hydrogen bonds, with little or no influence of the dynamic covalent bonds. In our previous work, we used tunable C═N bonds and metal-terpyridine bis-complexes as cross-links to prepare a series of IPN hydrogels with various rheological behaviors.[15] We also studied how these IPN hydrogels can disentangle and partially relax if one of the sub-networks is composed of cross-links with a shorter lifetime, e.g., combining oxime with zinc(II)-terpyridine bis-complexes or acylhydrazone with iron(II)-terpyridine bis-complexes. The results revealed that the partial relaxation of such IPNs takes place through a sticky Rouse relaxation process.

Herein, we investigate the viscoelastic properties of double dynamics networks of different topologies: the DCN, IPN, and DN, which are cross-linked by the same couple of interactions, i.e., reversible C═N bonds and metal-terpyridine bis-complexes. In this way, we will be able to systematically compare and discuss the interplay and possible synergetic effects between network topology and the characteristics of the two types of cross-links. Moreover, for each case, a comparison is made with the corresponding single networks to further

https://doi.org/10.1021/acs.macromol.2c00712
Macromolecules XXXX, XXX, XXX−XXX

Table 1. Main Characteristics of Copolymers

	final ratio[a] (mol %)						N_f/chain[d]	
copolymer	Tpy	ketone	DMA	M_n[b] (g/mol)	M_n[c] (g/mol)	$Đ$[c]	Tpy	ketone
P(T_2K_2)-S	1.6	2.2	96.2	54,100	53,700	1.37	8	11
P(T_2)-S	1.9		98.1	49,200	46,400	1.35	9	
P(K_2)-S		2.8	97.2	52,100	53,600	1.23		14
P(T_4)-S	3.2		96.8	54,100	53,200	1.36	16	
P(K_4)-S		4.0	96.0	51,000	58,300	1.34		20
P($K_{0.4}$)-L		0.4	99.6	262,000	171,000	1.58		10

[a]Calculated from the ^{1}H NMR spectra. [b]Evaluated by monomer conversion (^{1}H NMR). [c]Determined by SEC (polymethylmethacrylate standards). [d]Average number of functional groups per chain.

highlight the specific contribution of the different topologies to the network properties. To have a clear contrast of dynamics, we selected oxime bonds and zinc(II)-terpyridine bis-complexes as the two cross-linkers. The oxime bond was selected because of its weak dynamic character and high hydrolytic stability compared to other C═N bonds (e.g., semicarbazone, acylhydrazone, and imine).[35,36] Oxime-based cross-links are thus stable under the used conditions and will preserve the network integrity under shear stress. The zinc(II)-terpyridine bis-complexes (Zn^{2+}-Tpy) were used to provide dynamic properties to the networks due to their highly labile character.[37−39]

To reach our goal, we synthesized a series of terpyridine (Tpy) and/or ketone-functionalized hydrophilic poly(*N*,*N*-dimethyl acrylamide) (PDMA) random copolymers by reversible addition-fragmentation chain transfer (RAFT) controlled radical polymerization. Five "short-chain" (M_n approximately 50 kDa) copolymers were obtained that can be cross-linked with Zn^{2+}, to form zinc(II)-terpyridine bis-complexes, and/or with bis-hydroxylamine to form oxime bonds. Based on these, a DCN and two IPN hydrogels were prepared, as described in Figure 1. In addition, one of the above Tpy-functionalized copolymers was blended with a long-chain (M_n approximately 260 kDa) copolymer bearing a low density of ketone groups to prepare a DN hydrogel (Figure 1). To understand the role of each sub-network, the corresponding single networks were also prepared with the same copolymer compositions and concentrations but by cross-linking only one type of bond. By comparing the rheological behaviors of the prepared DCN, IPN, and DN hydrogels as well as their corresponding single networks, we determined the respective contributions of the two single networks (cross-linked by Zn^{2+}-Tpy or oxime) and investigated the effect of network topology on the viscoelastic properties. These results revealed that the formation of IPN and DN networks is influenced by a "screening" effect caused by the presence of un-cross-linked chains of the other copolymer type, which increases the proportion of ineffective intrachain associations. Nevertheless, the final hydrogels based on both Zn^{2+}-Tpy and oxime bonds have higher elasticity than the simple sum of the moduli of the corresponding single networks. Moreover, independently of their composition, the partial relaxation of all hydrogels was observed to start at a specific characteristic time, corresponding to the exchange/dissociation time of the labile Zn^{2+}-Tpy. Strain sweeps revealed that, whatever the network topology, the amplitude of deformation at which the linear viscoelastic region of the double dynamics networks stops is similar to the one of the corresponding single oxime networks, while the metallo-supramolecular network governs the amplitude of deformation up to which the sample can resist before starting to break.

RESULTS AND DISCUSSION

Synthesis of Functionalized Copolymers. The building blocks of the different hydrogels are water-soluble functionalized random copolymers with determined molar masses that were prepared by RAFT polymerization (see the Supporting Information). *N*,*N*-Dimethyl acrylamide (DMA) was selected as the base monomer for constituting the hydrophilic backbone of the copolymers. The commercially available diacetone acrylamide (DAAM) monomer was used to create oxime-based cross-links owing to the reaction between the ketone group of DAAM and the hydroxylamine group of the *O*,*O*′-(propane-1,3-diyl)bis(hydroxylamine) cross-linker. The terpyridine-functionalized monomer *N*-(3-([2,2′,6′,2″-terpyridin]-4′-yloxy)propyl)-*N*-methylacrylamide (TPy-AM) was synthesized (see the Supporting Information) and served as handles for the formation of zinc(II)-terpyridine bis-complexes (Zn^{2+}-Tpy) cross-links.

Six copolymers were thus obtained by varying ratios of functionalized monomers and will be combined differently to yield the desired hydrogels of varying topologies. All copolymers were characterized by ^{1}H NMR spectroscopy (see the Supporting Information) and size-exclusion chromatography (SEC) (Table 1).

Preparation of Hydrogels and Networks. For all the prepared networks, the amount of added cross-linkers (Zn^{2+} or bis-hydroxylamine) was half an equivalent compared to the reaction sites (terpyridine groups or ketone groups) of the corresponding functional copolymers unless otherwise stated, corresponding thus to the stoichiometric ratio to form bis-terpyridine metal complexes or oxime bonds. To enable comparisons between the different topologies shown in Figure 1, the polymer concentration used is such that at least one type of cross-link (Zn^{2+}-Tpy or oxime) in a given system leads to the formation of a hydrogel, i.e., the polymer concentration used for at least one type of cross-link is higher than the gel point. Specifically, the copolymer P(T_2K_2)-S was used as the precursor for preparing a DCN hydrogel and the corresponding single-cross-linked networks, i.e., networks cross-linked by only one type of bond (Zn^{2+}-Tpy or oxime) at 10 wt % polymer concentration (Scheme S6). Three IPN hydrogels were then prepared by mixing a copolymer bearing ketone groups and a copolymer bearing terpyridine groups. Two IPN1 hydrogels were obtained from the approximately 2% terpyridine-functionalized P(T_2)-S and the 2% ketone-functionalized P(K_2)-S copolymers (Schemes S7a and S8a). The first IPN1 was prepared at 10 wt % total concentration (5 wt % of each copolymer) and the second IPN1 at 20 wt % total

https://doi.org/10.1021/acs.macromol.2c00712
Macromolecules XXXX, XXX, XXX−XXX

concentration. The IPN1 hydrogels have similar strand length between the same types of cross-links as the DCN hydrogel (as can be seen from Table 1 and as illustrated in Figure 1). The IPN2 hydrogel was prepared at 10 wt % polymer total concentration from the same kind of copolymer but bearing approximately 4 mol % of functional groups ($P(T_4)$-S and $P(K_4)$-S) (Scheme S9a) to reach a comparable functional group concentration at the same total polymer concentration as the DCN hydrogel (10 wt %). The corresponding single networks were also prepared from the mixed solutions of the two copolymers, but only one of the copolymers was cross-linked with the appropriate cross-linker (Schemes S7b, S8b, and S9b). Finally, as shown in Scheme S10, the DN hydrogel was prepared from the short-chain $P(T_4)$-S and the long-chain ~0.4 mol % ketone-functionalized copolymers ($P(K_{0.4})$-L, with a M_n of approximately 260 kg/mol). In the DN hydrogel, the densely cross-linked and labile Zn^{2+}-Tpy network serves as the first (sacrificial) network, while the sparsely cross-linked and stable oxime network acts as the second network.[40] The corresponding single networks were also prepared by cross-linking only one copolymer of the mixture (Scheme S10b). The compositions of the different double dynamics networks are summarized in Table 2.

Table 2. Compositions of the Dual, Interpenetrated, and Double Networks

sample name	copolymer bearing Tpy groups and its weight fraction	copolymer bearing ketone groups and its weight fraction
DCN (10 wt %)	$P(T_2K_2)$-S (10 wt %)	
IPN1 (5 + 5 wt %)	$P(T_2)$-S (5 wt %)	$P(K_2)$-S (5 wt %)
IPN1 (10 + 10 wt %)	$P(T_2)$-S (10 wt %)	$P(K_2)$-S (10 wt %)
IPN2 (5 + 5 wt %)	$P(T_4)$-S (5 wt %)	$P(K_4)$-S (5 wt %)
DN (5 + 10 wt %)	$P(T_4)$-S (5 wt %)	$P(K_{0.4})$-L (10 wt %)

To promote cross-linking reactions and get stable and reproducible networks, an aging time of 2 days at 55 °C was applied followed by a slow cooling down to room temperature for another 2 days, for all networks, after the needed cross-linkers were added. By using such an aging procedure, gelation behaviors of DCN, IPN1, IPN2, and DN as well as their single networks have been tested by the tube inversion method, and the results are illustrated in Figure S1. Among these, 5 wt % $P(K_2)$-S in IPN1-Oxime (5 + 5 wt %), 5 wt % $P(T_4)$-S in IPN2-Zn^{2+}-Tpy (5 + 5 wt %), and 10 wt % $P(K_{0.4})$-L in DN-Oxime (5 + 10 wt %) were the gel points of the respective systems. As shown in Figure S1b, the IPN1-Zn^{2+}-Tpy (5 + 5 wt %) single network was not a gel; hence, a IPN1 at 10 + 10 wt % polymer concentration was also prepared as well as its two single networks (Figure S1c). The other single networks have polymer concentrations higher than their gel points. Since the different hydrogels are prepared directly from polymers, we decided to work in a rather low concentration regime to avoid preparation problems and favor good mixing and inter-penetration of the sub-networks.

Rheological Characterization. To investigate the contribution of the two types of cross-links to the dynamics (viscoelasticity) of the hydrogels of different topologies and of the corresponding single networks, oscillatory shear rheology in the linear viscoelastic (LVE) regime was used as the main characterization tool (see the Supporting Information for full details). As mentioned above, an aging protocol of 4 days (2 days at 55 °C followed by a slow cooling down to room temperature for another 2 days) was applied during the hydrogel preparation to obtain reproducible results. As shown in Figure S2a, the rheological behavior of the single oxime network did not change significantly after an additional 4 months of aging, indicating that a stable state has been reached during the aging protocol of 4 days. This result also suggests that our preparation protocol is sufficient to obtain stable Zn^{2+}-Tpy networks since the formation rate constant of oxime is lower than Zn^{2+}-Tpy at 25 °C in neutral water.[15] In addition, the samples were placed between the parallel plates of the rheometer for at least 15 min to equilibrate the samples before any experiments were performed (see the Supporting Information). As can be seen in Figure S2b, the data from the frequency sweeps performed after 15 and 30 min of resting for the single oxime and Zn^{2+}-Tpy cross-linked samples are similar. This indicates that 15 min of standing prior to testing is sufficient to allow the samples to reach reproducible conditions. Strain sweeps were also recorded on the different samples (see the Supporting Information for details).

Before discussing the different types of double dynamics hydrogels, i.e., cross-linked by both Zn^{2+}-Tpy complexes and oxime bonds, we will first examine the rheological behaviors of the corresponding single networks, i.e., where both copolymers are mixed but only one is cross-linked, to better understand the relative contribution of each type of cross-link.

Zn^{2+}-Tpy Single Cross-Linked Networks. The oscillatory frequency sweeps measured from high to low frequency on the single networks cross-linked only by Zn^{2+}-Tpy metallo-supramolecular bonds are shown in Figure 2. The plateau

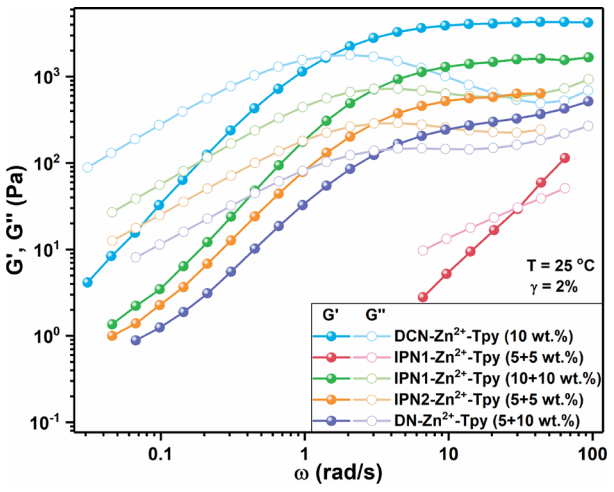

Figure 2. Comparison of oscillatory frequency sweeps on single Zn^{2+}-Tpy networks (see Table 3).

modulus values measured from these graphs as well as the characteristics of the copolymers and cross-linker concentrations used are summarized in Table 3. All single Zn^{2+}-Tpy networks, except the IPN1-Zn^{2+}-Tpy (5 + 5 wt %), showed similar evolution of the dynamic moduli with frequency. Since the diluted chains are unentangled (see Section S1.5 of the Supporting Information), it is expected that the observed elastic plateau comes from molecular segments trapped between two Zn^{2+}-Tpy complexes and that chains bearing

https://doi.org/10.1021/acs.macromol.2c00712
Macromolecules XXXX, XXX, XXX−XXX

Table 3. Compositions and Experimental and Theoretical Elastic Plateau Moduli of Different Single Zn^{2+}-Tpy Networks

sample name	copolymer used for Zn^{2+}-Tpy cross-links	[C][a] (mmol/L)	M_{xx}[b] (g/mol)	G'_p[c] (Pa)	$G^0_{N,\,theor}$[d] (Pa)	η_c[e] (%)
DCN-Zn^{2+}-Tpy (10 wt %)	P(T_2K_2)-S (10 wt %)	7.6	6700	4300	30,300	14
IPN1-Zn^{2+}-Tpy (5 + 5 wt %)	P(T_2)-S (5 wt %)	4.6	5400		19,200	
IPN1-Zn^{2+}-Tpy (10 + 10 wt %)	P(T_2)-S (10 wt %)	9.2	5400	1560	38,400	4.1
IPN2-Zn^{2+}-Tpy (5 + 5 wt %)	P(T_4)-S (5 wt %)	7.4	3300	630	34,100	1.8
DN-Zn^{2+}-Tpy (5 + 10 wt %)	P(T_4)-S (5 wt %)	7.4	3300	320	34,100	0.94

[a]The concentration of the added cross-linker (Zn^{2+}) is half of the Tpy concentration. [b]Number average molar mass between Tpy groups on the corresponding copolymer. [c]Obtained from the plateau value of G' in the high-frequency domain of the frequency sweeps. [d]Obtained based on eq 1. [e]Cross-linking efficiency (η_c), or probability for the stickers to form effective interchain cross-links, is calculated by $G'_p/G^0_{N,\,theor}$.

the Tpy groups along their backbone relax according to a sticky Rouse process.[41−43] The sample IPN1-Zn^{2+}-Tpy (5 + 5 wt %) does not form a gel (Figure S1b) because it contains a low concentration of the terpyridine bearing copolymer (5 wt %) with a low density of Tpy ligands (see Table 1), and its concentration is thus below the gel point. However, a gel is formed if the copolymer concentration is increased (see sample IPN1-Zn^{2+}-Tpy (10 + 10 wt %)) or if the density of Tpy ligands is increased (see sample IPN2-Zn^{2+}-Tpy (5 + 5 wt %)). Under these rather dilute conditions, it is expected that a large fraction of intrachain Tpy-Zn^{2+} complexes is formed.

As shown in Figure 2, the single network DCN-Zn^{2+}-Tpy (10 wt %) has the highest plateau modulus, suggesting that the DCN topology is more favorable to form effective Zn^{2+}-Tpy interchain linkages. This is confirmed by comparing its properties to the ones of IPN1-Zn^{2+}-Tpy (10 + 10 wt %), which has the same concentration of terpyridine bearing copolymer (10 wt %) and has a slightly larger concentration of cross-links (see Table 3). Despite this, the IPN1-Zn^{2+}-Tpy (10 + 10 wt %) sample exhibits a lower G' in the whole frequency range, indicating a lower density of elastically effective cross-links in this sample. For these systems, it is thus clear that the modulus value does not depend only on the sticker concentration. We attribute this reduction of effective cross-link density to a screening effect present in the IPN-derived single networks that is induced by the presence of the non-cross-linked copolymer.[15] The presence of free (non-cross-linked) polymer chains could reduce the probability of the terpyridine groups to find a partner to create an interchain junction and/or could reduce the solvent quality[44] (because of the higher total polymer concentration), which would also favor intrachain bond formation by decreasing the random coil size of the copolymer. The influence of the surrounding chains is probably enhanced by the fact that the concentration of the cross-linked copolymer is low. This implies that a very small variation in the association probability of the stickers can have a very large influence on the sample elasticity. This screening effect is also seen by comparing the viscoelastic response of the IPN2-Zn^{2+}-Tpy (5 + 5 wt %) and DN-Zn^{2+}-Tpy (5 + 10 wt %) single networks. For these two samples, the same P(T_4)-S copolymer at 5 wt % was used to form the Zn^{2+}-Tpy cross-linked single networks, which means that the polymer and cross-linker concentrations are identical. However, the storage modulus of the DN sample is lower than the one of the IPN over the whole frequency range, indicating that the addition of more free chains in the surroundings (10 wt % for DN versus 5 wt % for IPN) reduces further the formation of effective cross-links in the Zn^{2+}-Tpy network, providing further evidence that the presence of a non-cross-linked polymer does have a screening effect on the network formation.

It is also interesting to compare the DCN-Zn^{2+}-Tpy (10 wt %) and IPN2-Zn^{2+}-Tpy (5 + 5 wt %) single networks since both samples have very similar cross-linker concentrations but different concentrations in the cross-linked copolymer (Table 3). From the viscoelastic curves of Figure 2, it is clear that the DCN has a much higher plateau modulus. This large difference cannot be explained only by the screening effect and shows that, to obtain a larger elastic modulus, it is more favorable to have a large number of chains with few stickers than having a lower number of chains with more stickers. This result is in good agreement with ref 44, in which the authors show, based on simulations, that, in the semi-diluted regime, reducing the distance between stickers in a polymer chain favors the formation of intrachain associations. As already pointed out above, the polymer concentration is thus a key parameter for these systems.

The rubbery elastic plateau (G'_p) values[45,46] of the single Zn^{2+}-Tpy networks found experimentally are summarized in Table 3. As the dangling chain segments, which are not trapped in the network, are relaxing at very high frequency (outside the experimental window), this plateau modulus can be attributed to the contributions of molecular segments localized between two cross-links since they are unable to relax as long as the Zn^{2+}-Tpy complexes are associated.[37] If these trapped segments are entangled, then the sample elasticity is expected to be even larger. However, for all single Zn^{2+}-Tpy networks, the copolymer concentrations are rather low (Table 3). Therefore, the contribution of trapped entanglements may thus be considered as negligible, knowing that the average molar mass between two entanglements at a polymer concentration of 10 wt % is estimated at 110 kg/mol (see Section S1.5 of the Supporting Information). If we assume that all the functional groups of the copolymers are forming effective cross-links in the single networks, then the theoretical elastic plateau moduli G^0_N can be approximated by using the following equation:[15]

$$G^0_N = \frac{c\rho_0 RT}{M_{XX}}(1 - \varphi_{dangling}) \quad (1)$$

where ρ_0 is the density of PDMA in the melt state (approximated as 1 g/cm^3), c is the sample concentration, M_{xx} is the number average molar mass between two stickers, R is the universal gas constant, T is the temperature, and $\varphi_{dangling}$ is the weight fraction of dangling ends, which can be approximated as equal to $2M_{xx}/M_w$. The theoretical values of G^0_N are shown in Table 3 and compared to the G'_p values found experimentally. As a rough estimation of the cross-linking efficiency (or probability for the stickers to form effective interchain cross-links), the ratio of the experimental elastic plateau G'_p to the theoretical elastic plateau moduli G^0_N is also given. The cross-linking efficiency of all Zn^{2+}-Tpy single

https://doi.org/10.1021/acs.macromol.2c00712
Macromolecules XXXX, XXX, XXX−XXX

networks is rather low. As already mentioned, this can be understood by the low concentration of terpyridine-bearing copolymers, which promotes intrachain cross-linking, thus inducing ineffective internal loops.[37,47] The presence of unreacted sites is also probable. This is further shown by the fact that the two systems with the highest cross-linking efficiencies are the DCN and IPN1 (10 + 10 wt %), which have both the highest concentration in the active copolymer (10 wt %). As already mentioned, the significantly higher efficiency of forming Zn^{2+}-Tpy complexes in the DCN system than in the IPN and DN systems is attributed to the presence of a screening effect for IPN and DN systems, which limits the formation of effective interchain Zn^{2+}-Tpy linkages, while the DCN has no such effect. A similar conclusion can be drawn for the DN system, which has twice as much non-cross-linked ketone copolymer as the IPN2 system, while having the same concentration of Tpy copolymer and of Zn^{2+}, and has thus a more pronounced screening effect resulting in a significantly lower cross-linking efficiency.

Finally, all single Zn^{2+}-Tpy networks exhibit a similar terminal relaxation as shown by the G'-G'' crossover in Figure 2. Moreover, their relaxation process is close to a Maxwell-like behavior, characterized by a single relaxation time, τ_{st}. This relaxation process denotes the onset of macroscopic flow of Zn^{2+}-Tpy networks, mainly caused by the dissociation of Zn^{2+}-Tpy bis-complexes due to their rather low equilibrium constant and high lability.[9] According to ref 48, when the complexes start to dissociate, the sticky chains should relax by a sticky Rouse process, taking place from $\omega = 1/\tau_{st}$ to $\omega = 1/\tau = 1/\tau_{st}Z_{st}^2$, with Z_{st} being the number of active stickers along the chains. Such a process (during which G' and G'' scale with $\omega^{1/2}$) is not observed here. This is attributed to the very low number of stickers effectively active along the chains. From the very low level of the plateau modulus, it is indeed expected that most of the chains contain two or less active stickers.

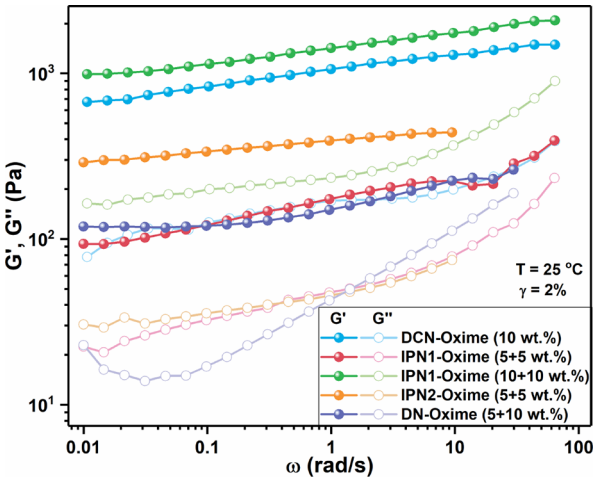

Figure 3. Comparison of oscillatory frequency sweeps of single oxime networks (see Table 4).

The accessible relaxation times (τ) of the single networks obtained from the crossover points of G' and G'' are presented in Table S2. Since the IPN1-Zn^{2+}-Tpy (5 + 5 wt %) did not form a gel, its G'-G'' crossover is barely measurable and this system shows thus the smallest relaxation time. The relaxation times of all the other IPN and the DN single networks are similar, suggesting that the lifetime of the stickers, τ_{st}, in these systems is very comparable (Table S2). The DCN-Zn^{2+}-Tpy (10 wt %) single network has the longest relaxation time (0.67 s) among all single networks. This result can be attributed to the higher density of active Zn^{2+}-Tpy cross-links in the DCN system.[49]

Oxime Single Cross-Linked Networks. The frequency sweeps recorded on the single oxime networks are shown in Figure 4. As expected, all single oxime networks are stable hydrogels as G' is mostly independent of the frequency and is larger than G'', showing an elastic response over the whole experimental frequency window. Table 4 presents the experimental plateau moduli (G'_p) and the theoretical plateau moduli (G_N^0) estimated by eq 1 for these single oxime networks.

It is obvious from Table 4 that, when the polymer concentration of the IPN1-Oxime systems increases from 5 to 10 wt %, the corresponding rubbery plateau value G'_p increases about 10 times, which is larger than a factor of 2 expected based on the change of concentration (for unentangled networks, G'_p scales linearly with the concentration, all other parameters being constant). This shows again that, for the lower concentrations, the network is at the limit of the gel formation, which leads to a large fraction of elastically inactive intrachain linkages and, consequently, to a high sensitivity of the oxime network to the polymer concentration. The importance of the concentration can also be seen on the cross-linking efficiencies (Table 4). Indeed, the three systems that have the highest concentration (10 wt %) of cross-linked copolymers (DCN, IPN1 (10 + 10 wt %), and DN) have all similar cross-linking efficiencies around 3%, while the two systems with a lower copolymer concentration (5 wt %) have much lower cross-linking efficiencies, below 1%.

The DCN-Oxime (10 wt %) and IPN1-Oxime (10 + 10 wt %) single networks have the same active copolymer concentration, but the IPN1 system has a larger concentration of cross-links (Table 4), as for the Zn^{2+}-Tpy single networks. However, contrary to the Zn^{2+}-Tpy single networks, the DCN-Oxime sample has a lower plateau modulus than IPN1-Oxime (10 + 10 wt %), and both systems have very similar cross-linking efficiencies. This is in stark contrast to the Zn^{2+}-Tpy single networks where the DCN system had a much higher plateau modulus and cross-linking efficiency (Table 3). This seems to indicate that, for the oxime single networks, the screening effect of the free chains is much less present than for the Zn^{2+}-Tpy single networks. To verify this point, we prepared an individual Zn^{2+}-Tpy network from pure P(T_2)-S and an individual oxime network from pure P(K_2)-S (Scheme S11). In such networks, there are thus no un-cross-linked chains of the other copolymer type. The individual networks were prepared at the same active copolymer concentration (10 wt %), as for the single networks, and their rheological behaviors were compared to the ones of the corresponding single networks derived from IPN1 (10 + 10 wt %) (Figure 4). The data of Figure 4 confirm that the screening effect is much less present for oxime-based networks than Zn^{2+}-Tpy networks since the difference in the modulus between single and individual networks is much less pronounced for oxime-based systems. This is also further confirmed by the cross-linking efficiency values, which are similar for individual and single oxime networks, while the cross-linking efficiency of the individual Zn^{2+}-Tpy network is much larger than the one of the single network (Tables 3 and 4 and Figure S3). The origin of

https://doi.org/10.1021/acs.macromol.2c00712
Macromolecules XXXX, XXX, XXX−XXX

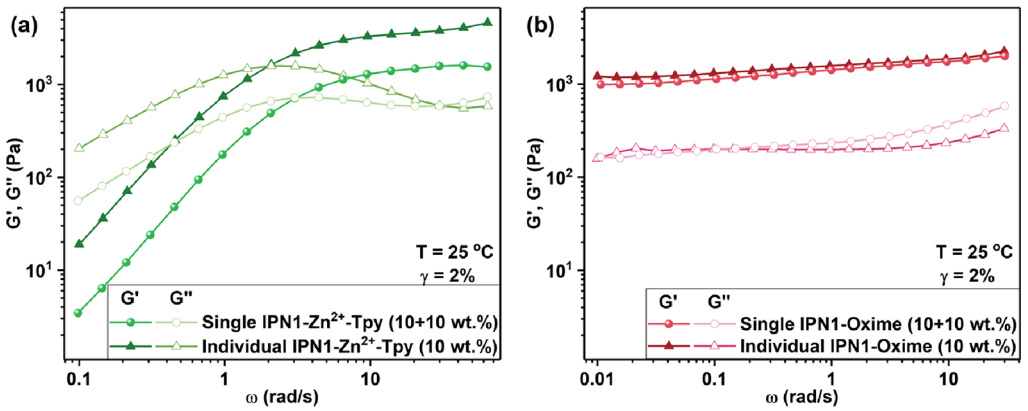

Figure 4. (a, b) Comparison between the oscillatory frequency sweeps performed on the individual Zn^{2+}-Tpy and oxime networks and on the single Zn^{2+}-Tpy and oxime networks.

Table 4. Compositions and Experimental and Theoretical Elastic Plateau Moduli of Single Oxime Networks

sample name	copolymer used for oxime cross-links	[C][a] (mmol/L)	M_{xx}[b] (g/mol)	G'_p[c] (Pa)	$G^0_{N,\,theor}$[d] (Pa)	η_c[e] (%)
DCN-Oxime (10 wt %)	$P(T_2K_2)$-S (10 wt %)	10.2	4900	1490	43,800	3.4
IPN1-Oxime (5 + 5 wt %)	$P(K_2)$-S (5 wt %)	6.9	3700	220	29,600	0.76
IPN1-Oxime (10 + 10 wt %)	$P(K_2)$-S (10 wt %)	13.8	3700	2080	59,200	3.5
IPN2-Oxime (5 + 5 wt %)	$P(K_4)$-S (5 wt %)	9.8	2500	440	45,900	0.96
DN-Oxime (5 + 10 wt %)	$P(K_{0.4})$-L (10 wt %)	2.0	26,200	230	8200	2.9

[a]The concentration of the added cross-linker (bis-hydroxylamine) is half of the ketone concentration. [b]Number average molar mass between ketone groups on the corresponding copolymer. [c]Obtained from the plateau value of G' in the high-frequency domain of the frequency sweeps. [d]Obtained based on eq 1. [e]Cross-linking efficiency (η_c), or probability for the stickers to form effective interchain cross-links, is calculated by $G'_p/G^0_{N,\,theor}$.

this difference in the screening effect between Zn^{2+}-Tpy and oxime single networks remains unclear.

As for the Zn^{2+}-Tpy networks, it is interesting to compare the DCN-Oxime (10 wt %) and IPN2-Oxime (5 + 5 wt %) single networks since both samples have very similar cross-linker concentrations but different active copolymer concentrations (Table 4). The much higher elastic modulus of the DCN single network shows again that it is more favorable to have fewer stickers but a large polymer concentration than having more stickers but a lower polymer concentration, in agreement with the results found for the Zn^{2+}-Tpy single networks.

A last observation on the DCN system must be highlighted: Comparing the data in Tables 3 and 4, we note that the rubbery plateau of the single oxime network (1490 Pa) is much lower than the corresponding rubbery plateau of the single Zn^{2+}-Tpy network (4300 Pa), despite the same copolymer concentration and a higher cross-linker concentration for the single oxime network. A possible explanation for this difference is the different kinetic and thermodynamic contributions of the two types of cross-links.[18,50−52] Indeed, Zn(II)-terpyridine bis-complexes are dynamic and allow for bond exchange. They have thus the possibility to correct defects during the 4 days of sample aging, leading to a better formed network and a higher plateau modulus.[39] On the other hand, oxime bonds are essentially inert under the conditions used here (as a reminder, no change was observed for the DCN single oxime network after 4 months of aging, see Figure S2), and there is thus no possibility for this system to correct connectivity defects such as loops and intramolecular associations, which are elastically inactive, leading to a lower plateau modulus than the single Zn^{2+}-Tpy network.[18] This is also confirmed by the rheological behavior of the individual networks derived from IPN1 (10 + 10 wt %) (Figure 4), where the plateau modulus of the Zn^{2+}-Tpy individual network is much higher than the one of the oxime individual network, despite the fact that the former has a lower cross-linker concentration (Table S3).

From the above discussions about Zn^{2+}-Tpy and oxime single networks, we can conclude that the labile Zn^{2+}-Tpy complexes allow for network relaxation over the observed time scales, while the stable oxime bonds allow the network to maintain a solid-like behavior over longer time scales. The labile Zn^{2+}-Tpy cross-links further impart a higher plateau modulus to the hydrogels than the oxime systems. The cross-linking efficiency of the copolymers is low in general because we work at a concentration close to the gel point and is strongly dependent on the copolymer concentration. In the case of Zn^{2+}-Tpy networks, it is also strongly affected by the presence of free copolymer chains, while this is much less the case for the oxime networks.

Double Dynamics Hydrogels Cross-Linked by both Zn^{2+}-Tpy and Oxime. Figure 5 shows the frequency sweeps of the five systems cross-linked by both Zn^{2+}-Tpy and oxime bonds. Whatever their topologies, all samples exhibit similar rheological behaviors, characterized by the presence of two elastic plateaus and a partial relaxation at intermediate frequency. The plateau in the high-frequency region can be attributed to both Zn^{2+}-Tpy and oxime cross-links, while the low-frequency plateau is governed by the oxime cross-links and appears after the fast reorganization of the network based on Zn^{2+}-Tpy complexes.[45] In addition, a characteristic slope of −0.5 is observed for the storage modulus in the transition region between the high-frequency and the low-frequency plateaus, indicating that this partial and slow relaxation of DCN, IPN, and DN hydrogels can be described by a Rouse process.[15] This relaxation process is attributed to the

https://doi.org/10.1021/acs.macromol.2c00712
Macromolecules XXXX, XXX, XXX−XXX

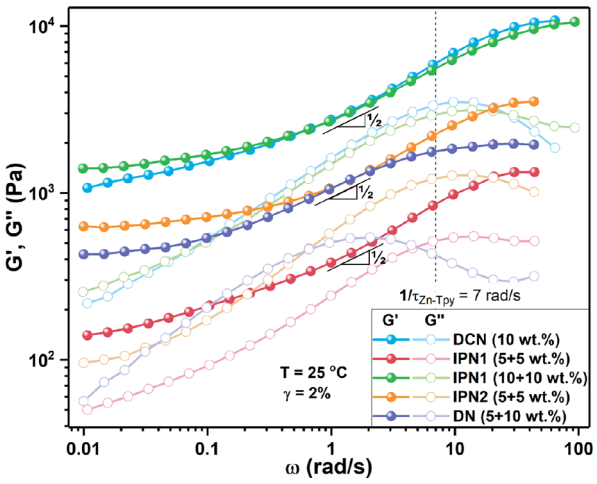

Figure 5. Oscillatory frequency sweeps on hydrogels of varying topology cross-linked by both Zn^{2+}-Tpy and oxime.

interpenetration of the two networks: As detailed in ref 15, the relaxation of the Zn^{2+}-Tpy networks (by a sticky Rouse process) is taking place at short times or high frequencies. The relaxation of the Zn^{2+}-Tpy network then leads to the partial relaxation of the oxime networks, which is well described by a constraint release Rouse process.[15,53]

Figure 6 and Table S4 compare the values of G'_p of the hydrogel systems cross-linked by both Zn^{2+}-Tpy and oxime

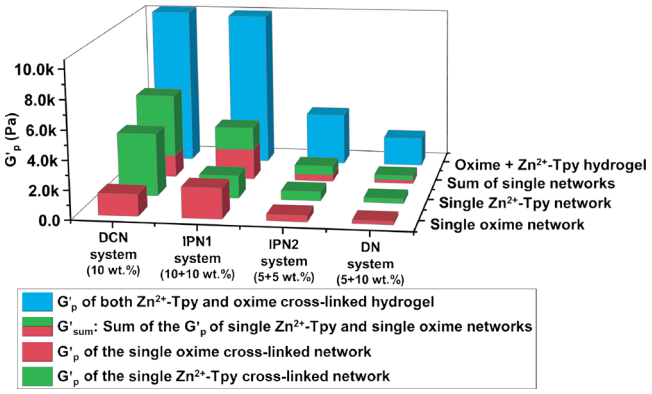

Figure 6. Summary of the plateau moduli for the DCN (10 wt %), IPN1 (10 + 10 wt %), IPN2 (5 + 5 wt %), and DN (5 + 10 wt %) systems including their corresponding single networks.

bonds and their two corresponding single networks. The sum (G'_{sum}) of the G'_p of the corresponding single Zn^{2+}-Tpy and oxime single networks and the ratio of G'_p/G'_{sum} of each system are also shown in Figure 6. Because the single IPN1-Zn^{2+}-Tpy at 5 + 5 wt % was not a gel and the plateau was not accessible in the measured frequency range, the IPN1 (5 + 5 wt %) system is not shown in the graph. It is clear from Figure 6 that the G'_p values of DCN, IPN, and DN hydrogels are much higher than the G'_{sum} of their single networks. However, the origin of this modulus increase is different according to the network topology. For the IPN and DN networks, the creation of new trapped entanglements between Zn^{2+}-Tpy and oxime networks, which serve as additional cross-links, is most probably the main factor responsible for the enhanced modulus of the hydrogels.[15,54] The situation is different for the DCN, which has both the Tpy and the ketone groups on the same chains. In this specific case, the main reason behind the enhanced modulus of the hydrogel is the low density of effective cross-links found for the single networks (see Tables 3 and 4), leading to a large weight fraction of dangling ends, which do not contribute to the sample elasticity. By allowing for the formation of both the oxime and the Zn^{2+}-Tpy bonds, the fraction of dangling ends is expected to be largely reduced. In particular, the chains containing only one active sticker in one of the single networks do not contribute at all to the sample elasticity; however, they are becoming active as soon as a sticker of the other nature is able to associate. Thus, in the specific case of the DCN network, there is a strong synergetic effect on the density of active stickers, rather than on the network interconnection as observed in the IPN and DN.

Figure 7 shows the comparison of the viscoelastic responses of the networks of different topologies to the ones of the single networks. From this comparison and from Figure 6, several observations can be made.

To further highlight the importance of the network topology, the modulus of the DCN (10 wt %) can be compared to the one of the IPN2 (5 + 5 wt %) system since they have very similar cross-linker concentration for both Zn^{2+}-Tpy and oxime and have the same total copolymer concentration. Despite these similarities, the G'_p value of IPN2 (3530 Pa) is approximately 3 times lower than that of the DCN (10,800 Pa). This large difference in the modulus has two possible origins. First, there could be a kind of cooperativity effect present only for the DCN topology. Indeed, unlike the IPN topology, the Tpy and ketone groups in the DCN are both on the same polymer chain, and the formation of one type of cross-link could thus ease the formation of the other types of cross-links. Second, the copolymer used for preparing the DCN sample has a larger average molar mass between stickers of the same nature, M_{xx}, than the copolymers used for IPN2 (Tables 3 and 4). A larger M_{xx} value decreases the probability to form intramolecular bonds, which are elastically inactive, and thus favors higher G' values.[44] Of course, this only applies if the concentration of cross-linkers is large enough to ensure that the chains contain several stickers.

Furthermore, as seen in Figure 7, the viscoelastic responses of the DCN and of the IPN1 (10 + 10 wt %) samples are very similar (both in curve shape and modulus values) despite their different characteristics. IPN1 (10 + 10 wt %) has indeed a twice higher total copolymer concentration and higher cross-linker concentrations for both Zn^{2+}-Tpy and oxime (see Tables 3 and 4). The low-frequency plateau of the DCN sample is slightly lower than IPN1 (10 + 10 wt %), which is in good agreement with the results found by comparing the corresponding single oxime networks, which was attributed to the lower cross-linker concentration in the DCN. However, based on the corresponding single Zn^{2+}-Tpy networks, one could have expected a lower rubbery plateau for the IPN1 (10 + 10 wt %) since the cross-linking efficiency and the G'_p for its Zn^{2+}-Tpy single network are much lower than the ones for the DCN single network (see Table 3). The relatively larger increase in the plateau modulus for IPN1 (10 + 10 wt %) than the DCN may be explained by its higher concentration of chains (20 wt %), which strongly promotes the inter-penetration of the two networks and the creation of trapped entanglements between the interpenetrated networks (see above), therefore largely reinforcing the sample. Thus, the DCN topology is more efficient to yield stronger hydrogels at

https://doi.org/10.1021/acs.macromol.2c00712
Macromolecules XXXX, XXX, XXX−XXX

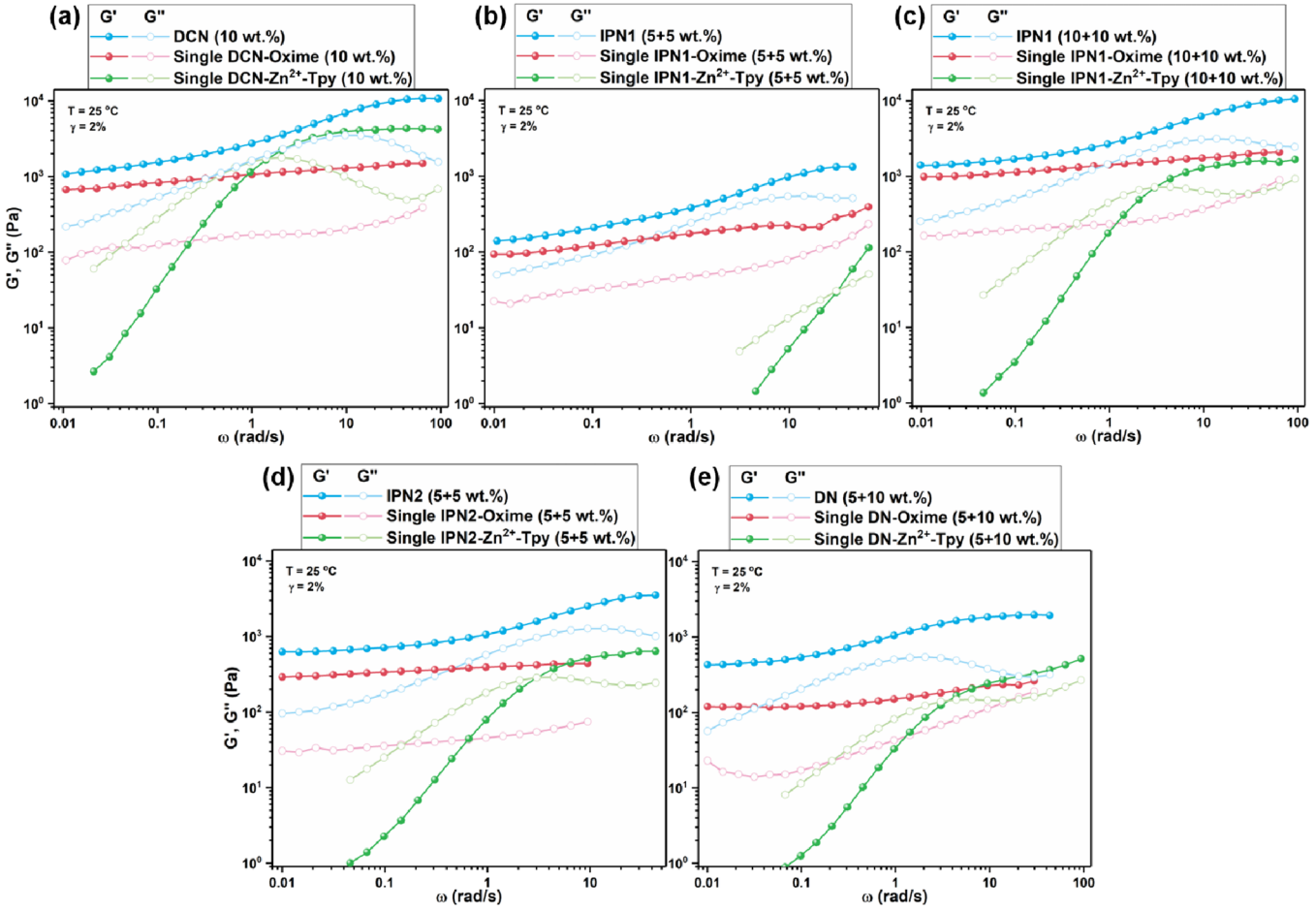

Figure 7. Oscillatory frequency sweeps on (a) DCN hydrogel and its single networks at 10 wt %, (b) IPN1 hydrogel and its single networks at 5 + 5 wt %, (c) IPN1 hydrogel and its single networks at 10 + 10 wt %, (d) IPN2 hydrogel and its single networks at 5 + 5 wt %, and (e) DN hydrogel and its single networks at 5 + 10 wt %.

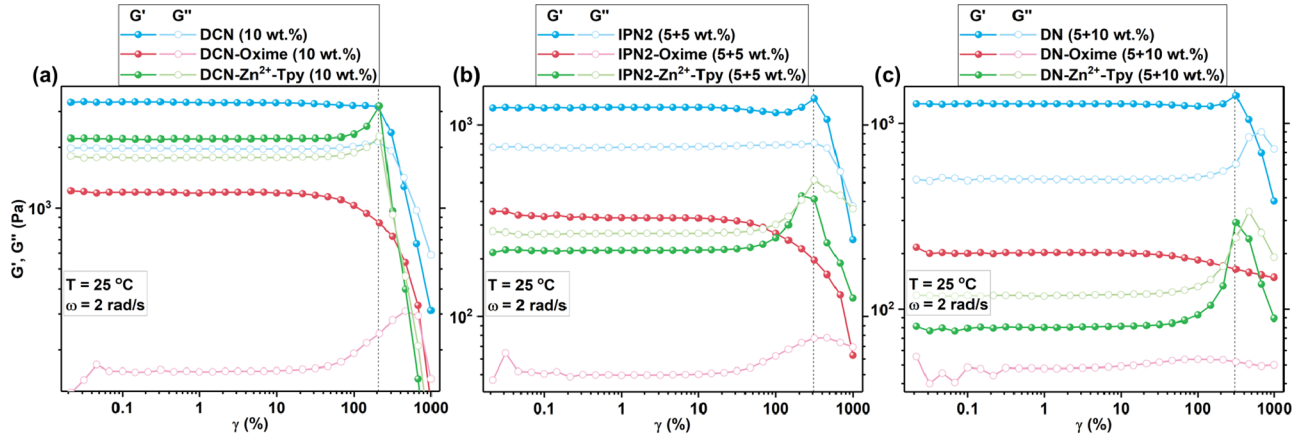

Figure 8. Oscillatory strain sweeps performed on the DCN (10 wt %) (a), on the IPN2 (5 + 5 wt %) (b), on the DN (5 + 10 wt %) (c), and on their corresponding single networks at a fixed frequency of 2 rad/s.

lower polymer and cross-linker concentrations (as it was shown for the single networks and from the comparison between the DCN and the IPN2 (5 + 5 wt %) samples, see above) but leads to a relatively lower synergetic effect of the two networks when compared to the more concentrated IPN1 (10 + 10 wt %). The positive influence of network interpenetration is also clearly visible in the viscoelastic response of the IPN1 (5 + 5 wt %) sample (Figure 7b). The corresponding single Zn^{2+}-Tpy network was indeed below the limit of gelation, but the IPN1 (5 + 5 wt %) hydrogel shows a well-developed rubbery plateau with a modulus value much higher than the single oxime network and containing thus a significant contribution from the Zn^{2+}-Tpy network.

In Figure 7, it is also observed that, whatever the topology, the low-frequency plateau modulus of the hydrogels is always higher than that of the corresponding single oxime network

https://doi.org/10.1021/acs.macromol.2c00712
Macromolecules XXXX, XXX, XXX−XXX

when the Zn^{2+}-Tpy network is fully relaxed in the low-frequency domain. This suggests that the process of DCN, IPN, and DN formation can also increase the cross-link density of the oxime network, which may be due to the topological constraints caused by the rapid formation of the Zn^{2+}-Tpy network that help to bring incompletely cross-linked hydroxylamines and ketones closer to each other.[37]

Influence of the Strain Amplitude on the Network Properties. To further probe the contributions of Zn^{2+}-Tpy and oxime cross-links to the DCN, IPN, and DN hydrogel mechanical deformation under strain, we performed amplitude strain sweeps on DCN (10 wt %), IPN2 (5 + 5 wt %), and DN (5 + 10 wt %) hydrogels as well as on their single networks. The IPN2 and DN systems are indeed sharing the same P(T_4)-S copolymer at the same concentration (5 wt %), and they have approximately the same concentrations of Zn^{2+} cross-linker as the DCN (10 wt %) system (Table 3). These strain sweeps were carried out at fixed frequencies of 0.2, 2, and 20 rad/s, i.e., frequencies at which the dissociation/association dynamics of the Zn^{2+}-Tpy cross-links can be considered as fast, possible, or slow, respectively (Figure 3). While all the strain amplitude sweep data are presented in Figures S3−S5, Figure 8 shows the viscoelastic response of the three systems deformed at a frequency of 2 rad/s.

As presented in Figure 8 and Figures S3−S5, in all measured strain sweeps, the linear viscoelastic regime of all single Zn^{2+}-Tpy networks is slightly more extended than the one of all single oxime networks. However, the strain that marks the transition of the gels from a solid-like to a liquid-like state at the critical G'-G'' crossover point of single oxime networks is always higher than that of single Zn^{2+}-Tpy networks at the same frequencies. The different behavior of the two types of single networks is due to several reasons. First, one can observe that the solid-to-liquid transition of the single oxime networks takes place gradually, with no sharp transition in the decrease in their storage modulus. Despite the very long lifetime of these networks in the linear regime, no signature of stretch is observed in their strain sweep data, which suggests that the structure of these networks is able to gradually adapt to the increasing deformation. However, while we could attribute this slow decrease in the storage modulus to the gradual breaking of the dynamic covalent bonds, it could also be due to the low cross-linking density of the oxime network, giving rise to a sample formed by several cross-linked clusters able to move separately, as observed with soft colloidal systems.[55] Looking at the reverse strain-sweep measurements (see Figures S3−S5), which were conducted by increasing the strain to the maximum strain amplitude that can be reached without taking the risk to expel the samples from the geometries and then decreasing the strain amplitude for recovery, it can be seen that the G' of the single oxime networks is slightly lower than the initial value when the strain amplitude is returned to low values. However, this effect is small, and there is almost no hysteresis, suggesting that the oxime network can rapidly recover its initial structure. On the other hand, the nonlinear properties of the single Zn^{2+}-Tpy networks are very different. The interesting aspect is that all these networks show a, sometimes very strong, shear thickening effect at high shear amplitude. The origin of shear thickening in associative polymers has been intensively debated and is generally classified into two main categories: (i) chain stretching beyond the Gaussian range but the number of elastically active chains does not change during shear and (ii) increase in the number of elastically active chains by incorporation of free chains into the existing network.[56−59] In our case, the fact that the G' values generally return close to their initial values when the strain is decreased (see Figures S3−S5) suggests that the shear thickening is not due to the strain-induced formation of additional Zn^{2+}-Tpy cross-links but rather to the chain stretching.[59] Meanwhile, at lower strain amplitude, the dynamics of the metal−ligand junctions is fast enough to ensure that the network can constantly adapt to the deformation; this is not the case anymore at large strain amplitude, which requires that the sample equilibrates on a larger length scale, involving the concerted dissociation of a larger number of supramolecular junctions. At this stage, the network strands start to stretch and shear thickening is observed. Upon further increasing the amplitude of deformation, the network cannot withstand the high stretch anymore, and the sample breaks in a rather sharp way. As shown in Figure 8, a lower cross-link density, as it is the case for the DN hydrogel, leads to a larger ability of the network strands to stretch before breaking.

Looking at the viscoelastic properties of the DCN, IPN2, and DN hydrogels, it is first observed that their stable linear viscoelastic regions are similar to the ones of the corresponding single oxime networks. Indeed, their storage modulus starts to decrease at the same strain amplitude, even if this effect is much less pronounced than in the corresponding single oxime networks. Then, the shear thickening coming from the Zn^{2+}-Tpy network starts to dominate the data until the hydrogels break. The importance of the shear thickening is lower than in the single Zn^{2+}-Tpy networks. This is because the integration of both Zn^{2+}-Tpy and oxime cross-links in the hydrogels confers a higher cross-linking density to the hydrogels, leading to a higher elastic modulus but decreasing the ability of the network strands to deform. The maximum of the storage modulus, which is reached before the rupture of the networks, is located at the same strain amplitude for both the double dynamics networks and their corresponding single Zn^{2+}-Tpy networks (dotted line in Figure 8). We can therefore conclude that it is the metallo-supramolecular network that governs the amplitude of deformation up to which the sample can resist before starting to break.

At these high strain amplitudes, the data do not allow determining to which extent the oxime network is also broken, its contribution being weaker than the response of the broken hydrogels. However, the comparison between Figure 8a,b, and 8c allows highlighting the different behaviors of the DN hydrogel. At 2 rad/s, the value of the storage modulus is the same for both the IPN2 and the DN hydrogels, and the maximum of G' is reached at the same strain amplitude. This can be understood by the fact that they both contain the same Zn^{2+}-Tpy network. However, at large strain amplitude (>300%), while the loss modulus of the IPN2 hydrogel largely decreases, indicating the failure of the sample, the loss modulus of the DN hydrogel first increases to reach a maximum and then only starts to decrease. This behavior is attributed to its oxime network, which is able to resist larger deformation. Indeed, it is the only sample still displaying a solid-like behavior at 1000% of deformation due to its very low density of cross-links and the very large length of its network strands, which significantly increase its deformability. Similar conclusions can be drawn from Figures S3−S5, where the strain amplitude sweep tests are performed at higher frequency (20 rad/s). Under this high frequency, the DN hydrogel is the only

https://doi.org/10.1021/acs.macromol.2c00712
Macromolecules XXXX, XXX, XXX−XXX

sample that starts to break (amplitude determined by the maximum of G') at larger amplitude than the amplitude at which its corresponding single Zn^{2+}-Tpy network starts to break. This suggests that the DN hydrogel is able to withstand larger strain compared to its single components.

CONCLUSIONS

In this work, we investigated the viscoelastic properties of DCN, IPN, and DN hydrogels based on two orthogonal types of reversible bonds as cross-links: zinc(II)-terpyridine coordination bonds and oxime bonds. We compared the oscillatory mechanical properties and dynamic relaxation behavior of these three hydrogel types as well as their corresponding single networks cross-linked only by Zn^{2+}-Tpy or oxime bonds.

Concerning the single networks, we showed that the labile Zn^{2+}-Tpy complexes allow for network relaxation behavior over the observed time scales, while the stable oxime bonds allow the network to maintain a solid-like behavior over longer time scales. The Zn^{2+}-Tpy bonds have a relatively higher cross-linking efficiency and impart thus a higher plateau modulus to the single networks than the oxime systems. The DCN, IPN, and DN hydrogels all exhibit similar rheological behaviors, characterized by the presence of two elastic plateaus and a partial relaxation at intermediate frequency. The high-frequency plateau is attributed to both Zn^{2+}-Tpy and oxime cross-links, while the low-frequency plateau is governed by the oxime cross-links and appears after the fast dissociation of Zn^{2+}-Tpy complexes. A characteristic slope of −0.5 was observed for the storage modulus in the transition region between the high- and low-frequency plateaus, indicating that this partial and slow relaxation can be described by a Rouse process.

The detailed comparison of the viscoelastic behaviors of the DCN, IPN, and DN hydrogels revealed that they have all higher elasticity than the simple sum of the moduli of the corresponding single networks. However, the origin of this modulus increase is different according to the considered topologies. For the DCN network, there is a strong synergetic effect based on the density of active stickers, while for the IPN and DN hydrogels, the creation of new trapped entanglements between Zn^{2+}-Tpy and oxime networks, which serve as additional cross-links, is the main factor responsible for the enhanced modulus. Strain sweeps revealed that, whatever the network topology, the stable linear viscoelastic region of the double dynamics networks is similar to the one of the corresponding single oxime networks, while the metallo-supramolecular sub-network governs the amplitude of deformation up to which the sample can resist before starting to break. A shear thickening coming from the Zn^{2+}-Tpy sub-network was also observed in all the hydrogels.

In this paper, we systematically investigated the effect of three network topologies on the viscoelastic properties of hydrogels. The question of selecting the most appropriate network topology for the desired application may arise for any hydrogel system when introducing two or more dynamic bonds but has rarely been discussed systematically in previous works. Our results show that topology does not significantly affect the lifetime of the metallo-supramolecular junctions. However, topology strongly influences the elastic modulus of the hydrogels and determines the magnitude of modulus increase. We hope that this study will provide the readers with new insight on how to select the best topology and with ideas for designing other dynamic hydrogels based on different types of bonds with desired properties.

ASSOCIATED CONTENT

Supporting Information

The Supporting Information is available free of charge at https://pubs.acs.org/doi/10.1021/acs.macromol.2c00712.

Experimental section, full details on the syntheses, supplementary figures, and tables (PDF)

AUTHOR INFORMATION

Corresponding Authors

Evelyne van Ruymbeke − *Institute of Condensed Matter and Nanosciences (IMCN), Bio and Soft Matter Division (BSMA), Université catholique de Louvain, Louvain-la-Neuve B-1348, Belgium;* orcid.org/0000-0001-7633-0194; Email: evelyne.vanruymbeke@uclouvain.be

Charles-André Fustin − *Institute of Condensed Matter and Nanosciences (IMCN), Bio and Soft Matter Division (BSMA), Université catholique de Louvain, Louvain-la-Neuve B-1348, Belgium;* orcid.org/0000-0002-3021-5438; Email: charles-andre.fustin@uclouvain.be

Author

Hui Yang − *Institute of Condensed Matter and Nanosciences (IMCN), Bio and Soft Matter Division (BSMA), Université catholique de Louvain, Louvain-la-Neuve B-1348, Belgium;* Present Address: Shaanxi Key Laboratory of Biomedical Metal Materials, Northwest Institute for Nonferrous Metal Research, Xi'an 710016, PR China (H.Y.); orcid.org/0000-0001-6883-4632

Complete contact information is available at: https://pubs.acs.org/10.1021/acs.macromol.2c00712

Notes

The authors declare no competing financial interest.

ACKNOWLEDGMENTS

This project was partially funded by the French Community of Belgium through ARC project N°16/21-076. H.Y. acknowledges the China Scholarship Council for the support of PhD fellowship. E.v.R. is the Senior Research Associate of the FRS-FNRS.

REFERENCES

(1) Sun, H.; Zhao, Y.; Wang, C.; Zhou, K.; Yan, C.; Zheng, G.; Huang, J.; Dai, K.; Liu, C.; Shen, C. Ultra-Stretchable, Durable and Conductive Hydrogel with Hybrid Double Network as High Performance Strain Sensor and Stretchable Triboelectric Nanogenerator. *Nano Energy* **2020**, *76*, No. 105035.

(2) Zhuo, S.; Zhao, Z.; Xie, Z.; Hao, Y.; Xu, Y.; Zhao, T.; Li, H.; Knubben, E. M.; Wen, L.; Jiang, L.; Liu, M. Complex Multiphase Organohydrogels with Programmable Mechanics Toward Adaptive Soft-Matter Machines. *Sci. Adv.* **2020**, *6*, 1464.

(3) Ryan, K. R.; Down, M. P.; Banks, C. E. Future of Additive Manufacturing: Overview of 4D and 3D Printed Smart and Advanced Materials and Their Applications. *Chem. Eng. J.* **2021**, *403*, No. 126162.

(4) Li, S.; Zhou, X.; Dong, Y.; Li, J. Flexible Self-Repairing Materials for Wearable Sensing Applications: Elastomers and Hydrogels. *Macromol. Rapid Commun.* **2020**, *41*, 2000444.

(5) Matsuda, T.; Kawakami, R.; Namba, R.; Nakajima, T.; Gong, J. P. Mechanoresponsive Self-Growing Hydrogels Inspired by Muscle Training. *Science* **2019**, *363*, 504−508.

(6) Li, C.; Iscen, A.; Palmer, L. C.; Schatz, G. C.; Stupp, S. I. Light-Driven Expansion of Spiropyran Hydrogels. *J. Am. Chem. Soc.* **2020**, *142*, 8447−8453.
(7) Dong, M.; Shi, B.; Liu, D.; Liu, J. H.; Zhao, D.; Yu, Z. H.; Shen, X. Q.; Gan, J. M.; Shi, B. L.; Qiu, Y.; Wang, C. C.; Zhu, Z. Z.; Shen, Q. D. Conductive Hydrogel for a Photothermal-Responsive Stretchable Artificial Nerve and Coalescing with a Damaged Peripheral Nerve. *ACS Nano* **2020**, *14*, 16565−16575.
(8) Liang, R.; Wang, L.; Yu, H.; Khan, A.; Amin, B. U.; Khan, R. U. Molecular Design, Synthesis and Biomedical Applications of Stimuli-Responsive Shape Memory Hydrogels. *Eur. Polym. J.* **2019**, *114*, 380−396.
(9) Rossow, T.; Seiffert, S. Supramolecular Polymer Gels with Potential Model-Network Structure. *Polym. Chem.* **2014**, *5*, 3018−3029.
(10) Golkaram, M.; Loos, K. A Critical Approach to Polymer Dynamics in Supramolecular Polymers. *Macromolecules* **2019**, *52*, 9427−9444.
(11) Podgórski, M.; Fairbanks, B. D.; Kirkpatrick, B. E.; McBride, M.; Martinez, A.; Dobson, A.; Bongiardina, N. J.; Bowman, C. N. Toward Stimuli-Responsive Dynamic Thermosets through Continuous Development and Improvements in Covalent Adaptable Networks (CANs). *Adv. Mater.* **2020**, *32*, 1906876.
(12) Perera, M. M.; Ayres, N. Dynamic Covalent Bonds in Self-Healing, Shape Memory, and Controllable Stiffness Hydrogels. *Polym. Chem.* **2020**, *11*, 1410−1423.
(13) Chakma, P.; Konkolewicz, D. Dynamic Covalent Bonds in Polymeric Materials. *Angew. Chem., Int. Ed.* **2019**, *58*, 9682−9695.
(14) Qin, B.; Yin, Z.; Tang, X.; Zhang, S.; Wu, Y.; Xu, J. F.; Zhang, X. Supramolecular Polymer Chemistry: From Structural Control to Functional Assembly. *Prog. Polym. Sci.* **2020**, *100*, No. 101167.
(15) Yang, H.; Ghiassinejad, S.; Van Ruymbeke, E.; Fustin, C. A. Tunable Interpenetrating Polymer Network Hydrogels Based on Dynamic Covalent Bonds and Metal-Ligand Bonds. *Macromolecules* **2020**, *53*, 6956−6967.
(16) McBride, M. K.; Worrell, B. T.; Brown, T.; Cox, L. M.; Sowan, N.; Wang, C.; Podgorski, M.; Martinez, A. M.; Bowman, C. N. Enabling Applications of Covalent Adaptable Networks. *Annu. Rev. Chem. Biomol. Eng.* **2019**, *10*, 175−198.
(17) Nadgorny, M.; Collins, J.; Xiao, Z.; Scales, P. J.; Connal, L. A. 3D-Printing of Dynamic Self-Healing Cryogels with Tuneable Properties. *Polym. Chem.* **2018**, *9*, 1684−1692.
(18) Li, Y.; Zhu, C.; Dong, Y.; Liu, D. Supramolecular Hydrogels: Mechanical Strengthening with Dynamics. *Polymer* **2020**, *210*, No. 122993.
(19) Huang, Z.; Chen, X.; O'Neill, S. J. K.; Wu, G.; Whitaker, D. J.; Li, J.; McCune, J. A.; Scherman, O. A. Highly Compressible Glass-Like Supramolecular Polymer Networks. *Nat. Mater.* **2022**, *21*, 103−109.
(20) Thompson, C. B.; Korley, L. T. J. 100th Anniversary of Macromolecular Science Viewpoint: Engineering Supramolecular Materials for Responsive Applications-Design and Functionality. *ACS Macro Lett.* **2020**, *9*, 1198−1216.
(21) Wang, S.; Urban, M. W. *Nat. Rev. Mater.* **2020**, *5*, 562−583.
(22) Nele, V.; Wojciechowski, J. P.; Armstrong, J. P. K.; Stevens, M. M. Tailoring Gelation Mechanisms for Advanced Hydrogel Applications. *Adv. Funct. Mater.* **2020**, *30*, 2002759.
(23) Hu, X.; Zhou, J.; Daniel, W. F. M.; Vatankhah-Varnoosfaderani, M.; Dobrynin, A. V.; Sheiko, S. S. Dynamics of Dual Networks: Strain Rate and Temperature Effects in Hydrogels with Reversible H-Bonds. *Macromolecules* **2017**, *50*, 652−659.
(24) Rodin, M.; Li, J.; Kuckling, D. Dually Cross-Linked Single Networks: Structures and Applications. *Chem. Soc. Rev.* **2021**, *50*, 8147−8177.
(25) Yuan, Y.; Shen, S.; Fan, D. A Physicochemical Double Cross-linked Multifunctional Hydrogel for Dynamic Burn Wound Healing: Shape Adaptability, Injectable Self-healing Property and Enhanced Adhesion. *Biomaterials* **2021**, *276*, No. 120838.
(26) Li, Y.; Yang, L.; Zeng, Y.; Wu, Y.; Wei, Y.; Tao, L. Self-Healing Hydrogel with a Double Dynamic Network Comprising Imine and Borate Ester Linkages. *Chem. Mater.* **2019**, *31*, 5576−5583.
(27) Ahmadi, M.; Löser, L.; Fischer, K.; Saalwächter, K.; Seiffert, S. Connectivity Defects and Collective Assemblies in Model Metallo-Supramolecular Dual-Network Hydrogels. *Macromol. Chem. Phys.* **2020**, *221*, 1900400.
(28) Silverstein, M. S. Interpenetrating Polymer Networks: So Happy Together? *Polymer* **2020**, *207*, No. 122929.
(29) Ishikawa, S.; Iijima, K.; Matsukuma, D.; Asawa, Y.; Hoshi, K.; Osawa, S.; Otsuka, H. Interpenetrating Polymer Network Hydrogels via a One-Pot and in Situ Gelation System Based on Peptide Self-Assembly and Orthogonal Cross-Linking for Tissue Regeneration. *Chem. Mater.* **2020**, *32*, 2353−2364.
(30) Haque, M. A.; Kurokawa, T.; Gong, J. P. Super Tough Double Network Hydrogels and Their Application as Biomaterials. *Polymer* **2012**, *53*, 1805−1822.
(31) Sun, T. L.; Kurokawa, T.; Kuroda, S.; Ihsan, A. B.; Akasaki, T.; Sato, K.; Haque, M. A.; Nakajima, T.; Gong, J. P. Physical Hydrogels Composed of Polyampholytes Demonstrate High Toughness and Viscoelasticity. *Nat. Mater.* **2013**, *12*, 932−937.
(32) Fu, X.; Hosta-Rigau, L.; Chandrawati, R.; Cui, J. Multi-Stimuli-Responsive Polymer Particles, Films, and Hydrogels for Drug Delivery. *Chem* **2018**, *4*, 2084−2107.
(33) Cao, Z.-Q.; Wang, G.-J. Multi-Stimuli-Responsive Polymer Materials: Particles, Films, and Bulk Gels. *Chem. Rec.* **2016**, *16*, 1398−1435.
(34) Zhang, R.; Zhang, C.; Yang, Z.; Wu, Q.; Sun, P.; Wang, X. Hierarchical Dynamics in a Transient Polymer Network Cross-Linked by Orthogonal Dynamic Bonds. *Macromolecules* **2020**, *53*, 5937−5949.
(35) Xi, W.; Scott, T. F.; Kloxin, C. J.; Bowman, C. N. Click Chemistry in Materials Science. *Adv. Funct. Mater.* **2014**, *24*, 2572−2590.
(36) Xu, J.; Liu, Y.; Hsu, S.-H. Hydrogels Based on Schiff Base Linkages for Biomedical Applications. *Molecules* **2019**, *24*, 3005.
(37) Ahmadi, M.; Seiffert, S. Thermodynamic Control over Energy Dissipation Modes in Dual-network Hydrogels Based on Metal-ligand Coordination. *Soft Matter* **2020**, *16*, 2332−2341.
(38) Ahmadi, M.; Seiffert, S. Dynamic Model Metallo-Supramolecular Dual-Network Hydrogels with Independently Tunable Network Crosslinks. *J. Polym. Sci.* **2020**, *58*, 330−342.
(39) Xu, X.; Jerca, F. A.; Jerca, V. V.; Hoogenboom, R. Covalent Poly(2-Isopropenyl-2-Oxazoline) Hydrogels with Ultrahigh Mechanical Strength and Toughness through Secondary Terpyridine Metal-Coordination Crosslinks. *Adv. Funct. Mater.* **2019**, *29*, 1904886.
(40) Gong, J. P.; Katsuyama, Y.; Kurokawa, T.; Osada, Y. Double-Network Hydrogels with Extremely High Mechanical Strength. *Adv. Mater.* **2003**, *15*, 1155−1158.
(41) Hawke, L. G. D.; Ahmadi, M.; Goldansaz, H.; van Ruymbeke, E. Viscoelastic Properties of Linear Associating Poly(n-butyl acrylate) Chains. *J. Rheol.* **2016**, *60*, 297−310.
(42) Leibler, L.; Rubinstein, M.; Colby, R. H. Dynamics of Reversible Networks. *Macromolecules* **1991**, *24*, 4701−4707.
(43) Rubinstein, M.; Semenov, A. N. Dynamics of Entangled Solutions of Associating Polymers. *Macromolecules* **2001**, *34*, 1058−1068.
(44) Santra, A.; Dünweg, B.; Prakash, J. R. Universal Scaling and Characterisation of Gelation in Associative Polymer Solutions. *J. Rheol.* **2021**, *65*, 549−581.
(45) Czarnecki, S.; Rossow, T.; Seiffert, S. Hybrid Polymer-Network Hydrogels with Tunable Mechanical Response. *Polymer* **2016**, *8*, 82.
(46) Kim, S.; Regitsky, A. U.; Song, J.; Ilavsky, J.; McKinley, G. H.; Holten-Andersen, N. In situ Mechanical Reinforcement of Polymer Hydrogels via Metal-Coordinated Crosslink Mineralization. *Nat. Commun.* **2021**, *12*, 667.
(47) Xu, X.; Jerca, F. A.; Jerca, V. V.; Hoogenboom, R. Self-Healing and Moldable Poly(2-isopropenyl-2-oxazoline) Supramolecular Hy-

https://doi.org/10.1021/acs.macromol.2c00712
Macromolecules XXXX, XXX, XXX−XXX

drogels Based on a Transient Metal Coordination Network. *Macromolecules* **2020**, *53*, 6566−6575.
(48) Chen, Q.; Tudryn, G. J.; Colby, R. H. Ionomer Dynamics and The Sticky Rouse Model. *J. Rheol.* **2013**, *57*, 1441−1462.
(49) Schmolke, W.; Ahmadi, M.; Seiffert, S. Enhancement of Metallo-Supramolecular Dissociation Kinetics in Telechelic Terpyridine-Capped Poly(Ethylene Glycol) Assemblies in the Semi-Dilute Regime. *Phys. Chem. Chem. Phys.* **2019**, *21*, 19623−19638.
(50) Yesilyurt, V.; Ayoob, A. M.; Appel, E. A.; Borenstein, J. T.; Langer, R.; Anderson, D. G. Mixed Reversible Covalent Crosslink Kinetics Enable Precise, Hierarchical Mechanical Tuning of Hydrogel Networks. *Adv. Mater.* **2017**, *29*, 1605947.
(51) Tan, C. S. Y.; Agmon, G.; Liu, J.; Hoogland, D.; Janeček, E.-R.; Appel, E. A.; Scherman, O. A. Distinguishing Relaxation Dynamics in Transiently Crosslinked Polymeric Networks. *Polym. Chem.* **2017**, *8*, 5336−5343.
(52) Vidavsky, Y.; Buche, M. R.; Sparrow, Z. M.; Zhang, X.; Yang, S. J.; DiStasio, R. A., Jr.; Silberstein, M. N. Tuning the Mechanical Properties of Metallopolymers via Ligand Interactions: A Combined Experimental and Theoretical Study. *Macromolecules* **2020**, *53*, 2021−2030.
(53) Zhang, Z.; Chen, Q.; Colby, R. H. Dynamics of Associative Polymers. *Soft Matter* **2018**, *14*, 2961−2977.
(54) Zhang, X.; Vidavsky, Y.; Aharonovich, S.; Yang, S. J.; Buche, M. R.; Diesendruck, C. E.; Silberstein, M. N. Bridging Experiments and Theory: Isolating the Effects of Metal-Ligand Interactions on Viscoelasticity of Reversible Polymer Networks. *Soft Matter* **2020**, *16*, 8591−8601.
(55) Vlassopoulos, D.; Cloitre, M. Tunable Rheology of Dense Soft Deformable Colloids. *Curr. Opin. Colloid Interface Sci.* **2014**, *19*, 561−574.
(56) Wang, S.-Q. Transient Network Theory for Shear-Thickening Fluids and Physically Cross-Linked Systems. *Macromolecules* **1992**, *25*, 7003−7010.
(57) Marrucci, G.; Bhargava, S.; Cooper, S. L. Models of Shear-Thickening Behavior in Physically Cross-Linked Networks. *Macromolecules* **1993**, *26*, 6483−6488.
(58) Ma, S. X.; Cooper, S. L. Shear Thickening in Aqueous Solutions of Hydrocarbon End-Capped Poly(ethylene oxide). *Macromolecules* **2001**, *34*, 3294−3301.
(59) Xu, D.; Hawk, J. L.; Loveless, D. M.; Jeon, S. L.; Craig, S. L. Mechanism of Shear Thickening in Reversibly Cross-Linked Supramolecular Polymer Networks. *Macromolecules* **2010**, *43*, 3556−3565.

https://doi.org/10.1021/acs.macromol.2c00712
Macromolecules XXXX, XXX, XXX−XXX